Environ Sci Pollut Res (2017) 24:12608–12617
DOI 10.1007/s11356-016-7611-3

Advanced mortar coatings for cultural heritage protection. Durability towards prolonged UV and outdoor exposure

F. Pino[1] · P. Fermo[1] · M. La Russa[2] · S. Ruffolo[2] · V. Comite[2] · J. Baghdachi[3] · E. Pecchioni[4] · F. Fratini[5] · G. Cappelletti[1]

Received: 21 June 2016 / Accepted: 6 September 2016 / Published online: 1 October 2016

Abstract In the present work, two kinds of hybrid polymeric–inorganic coatings containing TiO_2 or SiO_2 particles and prepared starting from two commercial resins (Alpha®SI30 and Bluesil®BP9710) were developed and applied to two kinds of mortars (an air-hardening calcic lime mortar [ALM] and a natural hydraulic lime mortar [HLM]) to achieve better performances in terms of water repellence and consequently damage resistance. The two pure commercial resins were also applied for comparison purposes. Properties of the coated materials and their performance were studied using different techniques such as contact angle measurements, capillary absorption test, mercury intrusion porosimetry, surface free energy, colorimetric measurements and water vapour permeability tests. Tests were also performed to determine the weathering effects on both the commercial and the hybrid coatings in order to study their durability. Thus, exposures to UV radiation, to UV radiation/condensed water cycles and to a real polluted atmospheric environment have been performed. The effectiveness of the hybrid SiO_2 based coating was demonstrated, especially in the case of the HLM mortar.

Keywords Mortars · Hybrid coatings · Cultural heritage · Surface modification · Aging · Exposure

Responsible editor: Philippe Garrigues

Electronic supplementary material The online version of this article (doi:10.1007/s11356-016-7611-3) contains supplementary material, which is available to authorized users.

✉ P. Fermo
paola.fermo@unimi.it

✉ G. Cappelletti
giuseppe.cappelletti@unimi.it

[1] Dipartimento di Chimica, Università degli Studi di Milano, Via Golgi 19, 20133 Milan, Italy

[2] Dipartimento di Biologia, Ecologia e Scienze della Terra (DiBEST), Università della Calabria, Via Pietro Bucci, Cubo 12 B, Arcavacata di Rende, 87036 Cosenza, Italy

[3] College of Technology, Eastern Michigan University, Ypsilanti, MI, USA

[4] Dipartimento di Scienza della Terra, Università degli Studi di Firenze, Florence, Italy

[5] CNR—Istituto per la Conservazione e la Valorizzazione dei Beni Culturali, Sesto Fiorentino, Florence, Italy

Introduction

The environmental conditions (i.e. temperature, humidity and air pollution) can seriously affect the monumental stones and for this reason, conservation of historical buildings is nowadays an important issue. Among the main agents responsible for stones deterioration, atmospheric pollution seriously affects buildings materials (Doehne and Price 2010; Toniolo et al. 2015). Carbon, sulphur and nitrogen oxides together with aerosol particulate matter, such as smoke, provoke surface soiling (Zielecka and Bujnowska 2006; Quagliarini et al. 2012; Goffredo 2013). Actually, the main degradation product is calcium sulphate from the transformation of $CaCO_3$, induced by the reaction with the acids, i.e. sulphuric acid and nitric acid, contained in rain.

The presence of moisture can enhance the damaging activity primarily in the case of interior with a high intrinsic porosity. Polymeric materials have been widely studied as protective coatings to limit the process of deterioration of building materials exposed to the environment, due to condensed water, pollution and salts formation. Thus, the protection of the cultural heritage buildings and monuments by surface

treatment with polymers is a convenient practice to reduce maintenance problems. Their ability to form a protective layer on the monument surface limits the transport of different fluids from the surface to interior. However, the simultaneous fulfilment of protection efficiency, transparency, stability and durability both to climate alteration and to chemical/mechanical attacks is nowadays a challenge (Toniolo et al. 2015). Traditionally, acrylic and vinyl polymers, organosilicon compounds and fluorinated film forming agents have been applied to stone monuments as protective hydrophobic coatings against deterioration (Zielecka and Bujnowska 2006).

Moreover, in the last few years, oxide-based nanomaterials have been frequently applied for restoration and conservation of works of art. Karapanagiotis et al. (2014) have recently reported the first successful fabrication of a superhydrophobic, water repellent organically modified silica (ORMOSIL) gel that, avoiding nanoparticles, can be used for the protection of monuments. However, this innovative material cannot still guarantee the colour preservation of the treated artefacts (in particular in the case of porous stones). Thus, transparent and self-cleaning treatments, which ensure a better preservation of stone elements, should be obtained. Lately, both transparent-hydrophobic mixed polydimethylsiloxane (PDMS)–TiO_2–SiO_2 coatings and a SiO_2 nanoparticles enriched commercial waterborne mixture of silanes and siloxanes have been proposed, and no colour modification of marble/mortar surfaces have been observed after their application (Chatzigrigoriou et al. 2013; Cappelletti and Fermo 2016).

In our previous study (Cappelletti et al. 2015b) an air-hardening calcic lime mortar (ALM) and a natural hydraulic lime mortar (HLM) were used as representative substrates for historical mortars, and commercially available Si-based resins (Alpha®SI30 and Silres®BS16) were adopted as protective agents to give hydrophobicity features to the artificial stones. In particular, the effectiveness of the two commercial resins in reducing salt formation (sulphate and nitrate), induced by the interaction of the mortars with the atmospheric pollutants, was demonstrated in the case of the HLM mortar.

Here, the same mortars were used as substrates, and two inorganic/organic hybrid coatings (SiO_2 nanoparticles + alkylpolysiloxanes emulsion (Bluesil®BP9710) and nano-TiO_2 nanoparticles + Alpha®SI30) were applied to increase the hydrophobicity features with respect to that of the pure resins. The surface properties of the coatings and their performance as protective agents were studied using different techniques such as contact angle measurements, colorimetric measurements, capillary absorption, water vapour permeability tests and salt crystallization resistance. Finally, the durability and the effect of ageing caused by the prolonged exposure to controlled and real environmental conditions will be discussed in details.

Materials and methods

Mortars preparation

Samples of an ALM and a natural HLM were produced following the detailed procedure described in our previous work (Cappelletti et al. 2015b). Before any test, the substrates were previously seasoned for at least 3 months and then cut in the desired shape. ALM samples are white and brittle, whereas HLM samples are hard and brownish blocks.

Hydrophobic commercial resins

Two commercially available resins were used both to protect the substrates and to modify the wettability features of the pristine mortars. Alpha®SI30 (purchased by Sikkens) is a silicon-based solvent-borne resin already characterized in our previous works (Fermo et al. 2014). It was found to be composed by a mixture of a trimethoxysilane, with a quite long chain (i.e. iso-octyl) and a polydimethylsiloxane (PDMS). The present resin was applied as it is without any further dilution. Instead, Bluesil®BP9710 (by Bluestar Silicones) is a concentrated of O/W emulsion (phase volume, $\phi = 0.44$) with an alkylpolysiloxane oligomer base, designed to protect surfaces against moisture. It is stabilized by exploiting a nonionic emulsifier at alkaline pH (around 10). It was applied after a 1:11 dilution in water.

Hybrid coatings

The hybrid coatings were produced by addition of inorganic nanoparticles to the resins in order to obtain a modification on the surface roughness of the mortars. Only two combinations between resins and inorganic nanoparticles were achieved to ensure the compatibility among the different raw materials of the formulation.

SI30 TiO_2 hybrid was prepared by adding homemade TiO_2 nanoparticles to Alpha®SI30 resin. The titania synthesis was carried out by simple hydrolysis and polycondensation of a titanium alkoxide to obtain a transparent sol (Cappelletti et al. 2015a) stable for several weeks at room temperature and without any control of atmospheric humidity. According to our previous work (Maino et al. 2013), TiO_2 nanoparticles have uniform dimensions of about 20 nm. The mixture of the obtained titania sol and the siloxane polymeric agent (1:1 by weight) was stirred vigorously to obtain a homogeneous dispersion. The corresponding concentration of the TiO_2 sol was equal to 1.5 wt%.

Instead, BP9710 SiO_2 hybrid was obtained by mixing Bluesil®BP9710 with a transparent suspension of SiO_2 nanoparticles (LUDOX®LS, from Sigma-Aldrich, $\phi = 0.30$). The latter powders, electrostatically stabilized at pH 8, have an average particle size of 12 nm with a specific surface area of

220 m^2 g^{-1}. The final concentration of the silica nanoparticles in the hybrid formulation was 1 wt%.

The application of coatings on mortars surfaces was carried out by using a brush in a homogeneous manner in order to reproduce everyday working conditions. All the clad mortars were dried for 24 h in an oven at constant temperature (50 °C).

Sample characterizations

Water static contact angle (SCA) measurements of water on bare and coated mortars were performed on a Krüss Easy instrument. A drop of 6–10 μL, depending on the adopted solvents, was gently placed on the surface; the drop profile was extrapolated using appropriate fitting functions depending on the drop shapes. Measurements were repeated several times (>20) to obtain a statistical population especially for bare mortars, which were really variables even in near spots.

Scanning electron microscopy (SEM) was carried out using a SEM Hitachi TM-1000 Microscope.

Surface free energy (SFE) and the relative polar and disperse components were evaluated by using the Owens–Wendt–Rabel–Kaelble (OWRK) method (Owens 1969; Cappelletti et al. 2013) by using different high purity solvents (i.e. diiodomethane, glycerol, ethylene glycol, diethylene glycol).

Colorimetric measurements were performed to verify the colour modification of the protective films after both the deposition of the protective coatings and the various ageing tests (see in the following). The chromatic coordinates were calculated according to the Commission Internationale d'Eclairage (CIELab method) (Cappelletti et al. 2015b), starting from diffuse reflectance spectra acquired in the UV–Vis spectral range from 800 to 350 nm with a JASCO/UV–Vis/NIR spectrophotometer model V-570 instrument. According to the literature, no significant variation occurs when $\Delta E^* < 5$ (La Russa 2012; Esposito Corcione et al. 2014).

The water vapour permeability (WVP) of bare and coated mortars was evaluated by means of the methodology described in the European Standard Norma EN 15803 (UNI EN 15803 2009; Manoudis et al. 2009b).

Capillary water absorption measurements were performed on bare and coated materials by the gravimetric sorption technique, as described in the standard protocol UNI EN 15801 "Conservation of cultural property—test methods—determination of water absorption by capillarity" (UNI EN 15801 2010; Cappelletti et al. 2015b). Capillary absorption (CA) coefficient and capillarity index (CI; which gives information about the resistance to capillary rise when prolonged contact with water occurs) were determined, accordingly.

Porosity and pore size distributions were determined by mercury intrusion porosimetry (MIP), through a Micromeritics Autopore IV with a maximum pressure of 400 MPa, according to the procedure reported in a previous work of some of the co-authors of this paper (Ruffolo et al. 2014). Measurements were performed on samples with the same weight (1.5 g) to standardize testing and minimize errors. This technique allowed to determine pore sizes ranging from 0.003 to 40 μm.

Controlled ageing tests and exposure

Various ageing tests were performed to evaluate the stability of the protective coatings: (i) under UV irradiation (500 W halide lamp, 215–365 nm for 50 h, irradiance specific power of 45.5 mW cm^{-2}) and (ii) by using a Q-panel laboratory UltraViolet (QUV)/basic accelerated weathering tester, equipped with UVA-340 lamps (optimal sunlight conditions in the critical short wavelength region in the range 295–365 nm, irradiance specific power of 3.6 mW cm^{-2}) for a period of about 1000 h. This kind of test was used to simulate the critical conditions through cycles of moisture condensation and UV irradiation. Indeed, the controller in QUV test monitors UV intensity and compensates for lamp ageing or any other variability by adjusting power to the lamps. To simulate outdoor weathering, the QUV tester exposes materials to alternating cycles of UV light and moisture. Because materials can stay wet outdoors for an average of 8–12 h per day, it is difficult to accelerate moisture attack in a laboratory tester. The QUV moisture cycles were conducted at elevated temperatures to increase the severity and accelerate the damaging effects of moisture. In many outdoor environments, materials are wet more than 12 h each day; hence, the main cause of this outdoor wetness is dew. The QUV simulated this condition using an innovative condensation mechanism in which a water reservoir in the bottom of the test chamber is heated to produce vapour. The hot vapour maintains the chamber at 100 % relative humidity at elevated temperatures.

Finally, the samples were exposed in a typical urban environment in Milan. The exposure site was in the Milan University Campus, an area quite far from the city centre, which is considered representative of a typical urban background. The exposure tests were carried out for 7 months during winter (15 November 2014–15 May 2015). Ion chromatography (IC) was employed for the analysis of soluble salts (Cl^-, NO_3^- and SO_4^{2-}) in the exposed mortars. The samples were prepared according to a procedure reported elsewhere (Cappelletti et al. 2015b).

Results and discussion

Properties of bare and coated mortars

ALM and HLM substrates show a hydrophilic character ($\theta < 90°$) leading to the complete and almost immediate absorption of water drops. For this reason, the evaluation of the water static contact angles (Table 1, second column) has been

Table 1 Static contact angles (θ) and surface free energy (SFE, γ) values (with relative standard deviations) by Owens, Wendt, Rabel and Kaelble (OWRK) method with its polar component (γ_P)

Sample	θ/deg	γ/mN m^{-1}	γ_P/mN m^{-1}
ALM	70 ± 10	37 ± 7	13 ± 3
ALM SI30	116 ± 8	15 ± 6	<1
ALM SI30 TiO_2	129 ± 4	[a]	[a]
ALM BP9710	114 ± 7	12 ± 3	<1
ALM BP9710 SiO_2	126 ± 9	[a]	[a]
HLM	65 ± 10	33 ± 10	15 ± 5
HLM SI30	137 ± 7	<10	<1
HLM SI30 TiO_2	>150	[a]	[a]
HLM BP9710	130 ± 7	<10	<1
HLM BP9710 SiO_2	>150	[a]	[a]

The use of both nanoparticles resulted in elevated static contact angles (>150°) that varied in the range from 160° to 168°

[a] For hybrid coatings, the OWRK method was not applicable since θ > 120°

performed by using the first frames taken by the video registration of deposition procedure. Both the substrates were produced with the same coarse aggregate (0.5 mm < d < 4 mm) demonstrating an intrinsic variability, which is reflected in high standard deviations (Table 1). Moreover, SFE determination through the OWRK method leads to consistent values determining high polar surfaces for both the bare substrates (Table 1, third and fourth columns).

After the treatment with all the pure protective agents (Alpha®SI30 and Bluesil®BP9710), a successful hydrophobization of the substrates occurs (θ > 90°; Table 1, second column), as already pointed out in our previous work (Cappelletti et al. 2015b). Furthermore, these results are consistent with those recently reported in the literature: indeed, by applying several commercial siloxane/silane resins on different stone materials, hydrophobic coatings have been obtained, which are characterized by a maximum contact angle higher than 100° (Manoudis and Karapanagiotis 2009a; Chatzigrigoriou et al. 2013).

Particularly, both the hybrid coatings increase the surface hydrophobicity reaching the superhydrophobic properties only in the case of HLM substrate (Table 1, second column); hence, highlighting, once again, the pivotal role also played by the intrinsic variability of AL and HL mortars themselves. Figure S1 shows, in the case of SI30 TiO_2 coating (Fig. S1b), the increased roughness due to randomly distributed nano-

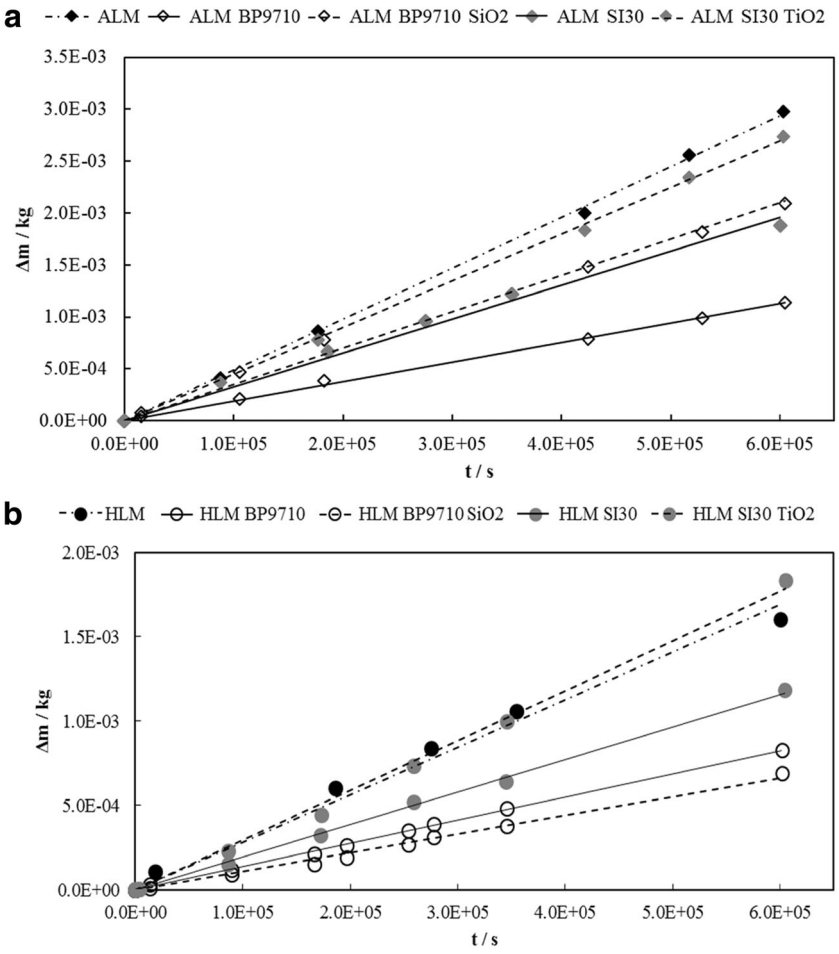

Fig. 1 Water vapour permeability curves showing the variation of cumulative mass for all the samples (both **a)** air-hardening calcic lime (AL) and **b)** hydraulic lime (HL) mortars)

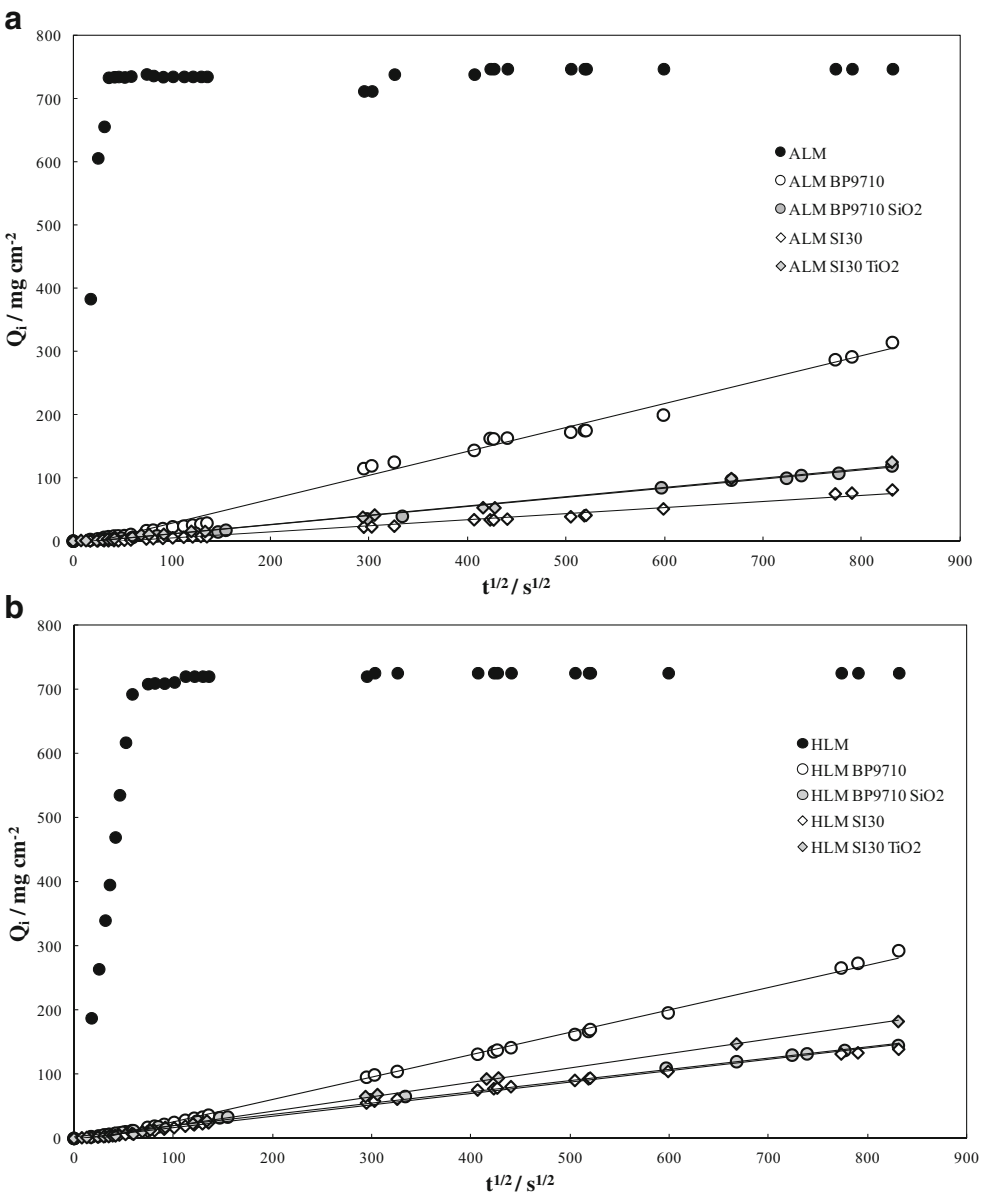

Fig. 2 Capillary absorption for **a)** air-hardening calcic lime (AL) and **b)** hydraulic lime (HL) mortars

titania aggregates on the ALM surface, which are responsible for the observed superhydrophobicity.

Furthermore, SFE evaluation, carried out for the samples treated with the commercial resins SI30 and BP9710, shows a drastic decrease in the polar component of the total surface free energy (Table 1, second column), as it was expected. On the contrary, for hybrid systems, it has not been possible to calculate the SFE, since contact angles with water and highly polar solvents could not be determined ($\theta > 150°$).

Thus, by comparing the performances of the two commercial resins, Alpha®SI30, as reported in our previous work, gave the best results especially when applied onto the hydraulic lime mortar, probably due either to the presence of an adequate micro-porosity (Cappelletti et al. 2015b) or to the different interaction with the resin in the presence of silicates (Fermo et al. 2014). Moreover, as concern the hybrid coatings performance, the combination of the intrinsic porosity of HLM with the nanoscale and microscale surface roughness (induced by the introduction of nanoparticles) has probably led to the superhydrophobicity features ($\theta > 150°$). This is an interesting result, especially for water-based system, since the environmental issues arising from the use of a solvent-borne system are a well-known drawback (Wicks 2007). Furthermore, all the protective coatings are invisible to naked eye ($\Delta E^* < 5$).

Moreover, since the water vapour transmission rate through the mortars must not be reduced after the coating treatments (Zielecka and Bujnowska 2006), a little change in the samples pore structure is an important result. In Fig. 1, as result of the WVP test, the cumulative mass change is shown

Table 2 Water capillary index (CI), absorption coefficient (CA) and amount of water absorbed at the final time (around 8 days, Q_{tf})

Sample	CI	CA/mg/cm^2 s$^{-1/2}$	Q_{tf}/s$^{1/2}$
ALM	0.97	17.24	747.4
ALM SI30	0.43	0.12	81.0
ALM SI30 TiO_2	0.51	0.08	77.0
ALM BP9710	0.46	0.21	314.2
ALM BP9710 SiO_2	0.51	0.10	119.1
HLM	0.96	11.45	725.0
HLM SI30	0.53	0.12	138.8
HLM SI30 TiO_2	0.49	0.09	144.3
HLM BP9710	0.46	0.37	292.2
HLM BP9710 SiO_2	0.53	0.13	144.6

($|\Delta m| = m_i - m_0$, where m_i and m_0 are the masses of the test assembly respectively at time t_i and t_0, in kg) for each set of successive weighing of the specimens versus time. Surprisingly, both the hybrid systems showed a better behaviour than the two commercial resins. Among the applied coatings, the smallest reduction in WVP was given by the hybrid SI30 TiO_2, which reaches a vapour flow comparable with that of the reference. The commercial silicon aqueous emulsion BP9710, applied on both mortars, showed a sensible reduction with respect to water vapour permeability, thus leading to a decrease that can be almost considered acceptable in materials transpiration (threshold value of 50 %; Rodrigues 2007; Cappelletti and Fermo 2016). Furthermore, this is fully in accordance with what is already reported in the literature for highly hydrophobic silane- and silicone-hybrid coatings, which are known to be able to maintain a high degree of water vapour permeability (Zielecka and Bujnowska 2006). Indeed, these resins allow stones to breathe and, at the same time, they prevent deterioration phenomena caused by external agents, such as atmospheric pollution (see in the following).

As commonly reported in the literature (Bortolotti et al. 2006; De Ferri et al. 2011), the prevention of water rising by capillary absorption plays a pivotal role in the conservation of historical buildings. This phenomenon is one of the main responsible of mortars degradation, since water freeze–thaw cycles can cause cracks, and the transport of salts inside the materials can lead to crusts formation. Figure 2 shows the amount of water absorbed per unit area over time (Q_i) for all the adopted mortars. Typical parameters of the present analyses, including CA and CI, are calculated and reported in Table 2. For the untreated mortars, the rise quickly arrives to a plateau that corresponds to the water saturation equilibrium of the sample. On the contrary, when the pure resins are applied on the mortars surface, a dramatic decrease in the capillary rise parameters (Table 2; Fig. 2) occurs for all of the treated substrates: the final Q_i collapses, CA reduces of about two orders of magnitude and CI is halved, confirming the hydrophobic performances of both the resins. Comparing the two commercial resins, Alpha®SI30 shows the best behaviour with both the types of mortars and the water absorption is

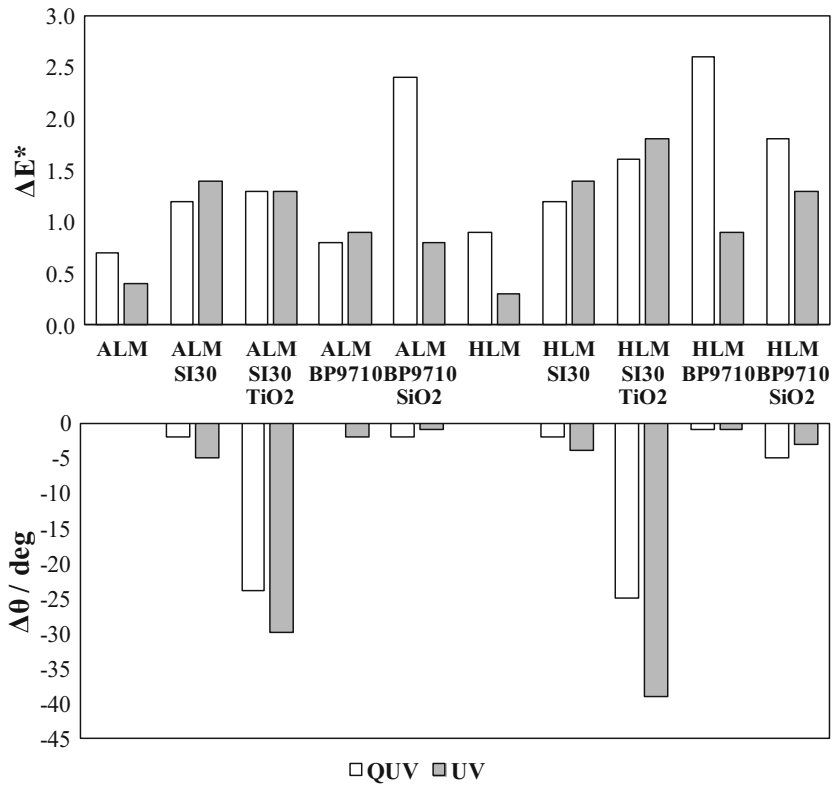

Fig. 3 ΔE^* (*above*) and static contact angle variations *(below)* after controlled accelerated ageing tests

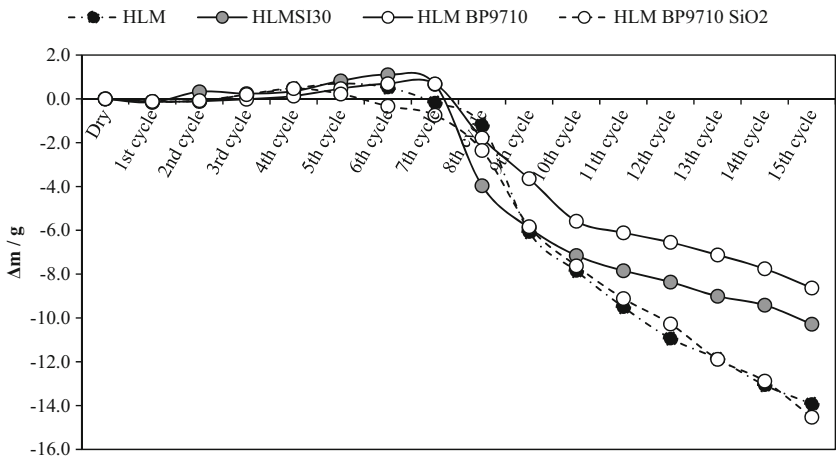

Fig. 4 Mass loss vs cycles number showing the resistance of the hydraulic lime mortar towards salt crystallization

further reduce in the corresponding hybrid systems. Commercial BP9710 shows, by contrast, an opposite behaviour: higher CA and Q_i values are obtained with pure resin, whereas the addition of silica nanoparticles strongly improve its performances, making it competitive with the solvent-based system. Overall, all the samples showed promising protective properties.

Controlled ageing tests and exposure

In order to evaluate the coatings stability, all the samples were treated both under direct UV lamp irradiations and in a QUV/basic machine for 1000 h accelerated ageing test (Figs. S2 and S3). The latter is equipped with UVA lamps, alternating 8 h of light with 8 h of water vapour condensation (in the dark). These conditions can reproduce well the ageing due to external physical agents, excluding the contribution of chemical reactions occurring in a polluted environment (Technical Bulletin LU-8010 1987; Technical Bulletin 1993; Fedor and Brennan 1996).

As shown in Fig. 3, all the samples show no significant ΔE^* variations after the ageing and only a slight loss of hydrophobicity has been observed, with exception of the SI30 TiO_2 hybrid coating, for which a significant decrease in the SCA values has been noticed for both the mortars. This fact could be easily explained considering the TiO_2 photoactivity, which could have promoted the degradation of the organic resin (Morikawa et al. 2006; Fujishima et al. 2008; Irie et al. 2009; Ohtani 2010; Kaur and Singh 2012). On the contrary, BP9710 SiO_2 has seemed to be well performing, since it shows both small ΔE^* and SCA variations.

Furthermore, the comparison between this kind of test and the UV ageing has shown that the main reason for coating deterioration is the UV light, whereas high humidity and condensation cycles seem not to affect the stability of the commercial and the hybrid coatings. Taking into account the lower power of the QUV lamp than the used halide lamp, the faster decrease in the SCA values of the UV irradiated samples can be easily explained (Fig. 3).

Another issue of interest in historical building is related to salt crystallization occurring into porous structure of the material, which exerts the so-called crystallization pressure on the pore walls leading to the degradation of the material. In this study, salt crystallization tests were performed in order to assess the effect of the treatment on the resistance against salt weathering (Flatt 2002; Wicks 2007; Yu and Oguchi 2010; La Russa 2012; Caruso et al. 2014). In Fig. 4, it has been reported the mass variation of samples after each weathering cycle. All specimens, after 3–5 cycles, showed an increase in weight related to the salt precipitation inside the pore structure. After the fifth–seventh cycles, all samples start to lose material. Treated specimens show a better behaviour since after 15 cycles, they suffer less variation of mass (ranging from 8 to 10 %). An exception is represented by HLM BP9710 SiO_2 sample; in this case, the behaviour against salt crystallization is quite similar to the untreated sample. In order to better understand the resistance of samples towards salt weathering, a calculation of the crystallization pressure has been performed from MIP measurement and applying a

Table 3 Mercury intrusion porosimetry parameters

Parameters		HLM	HLM BP9710	HLM BP9710 SiO_2	ALM	ALM BP9710	ALM BP9710 SiO_2
Porosity	%	23.3	23	22.8	28	27.7	27.6
Crystallization pressure	MPa	17.0	34.0	61.5	2.6	4.9	2.2

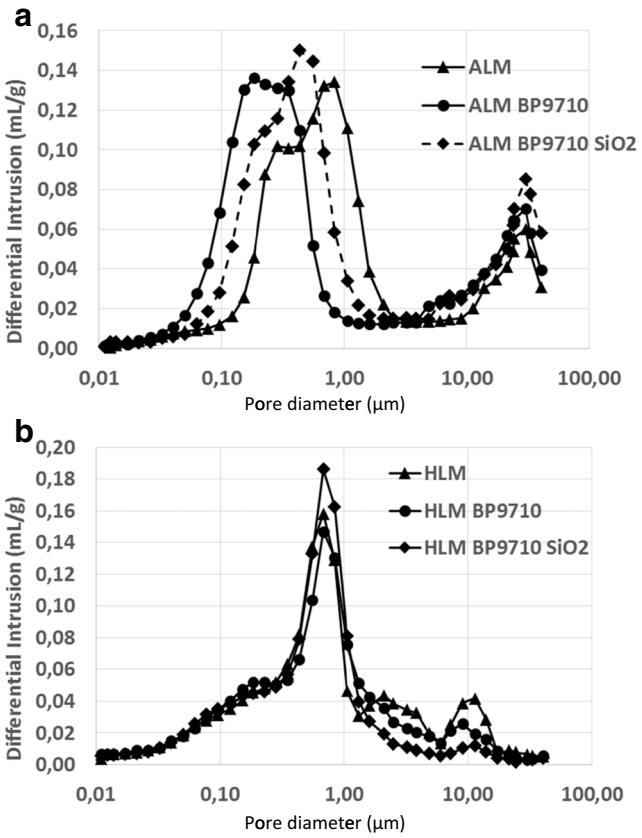

Fig. 5 Pore size distribution measured by means of mercury porosimetry (MIP) for **a)** air-hardening calcic lime (AL) and **b)** hydraulic lime (HL) mortars

thermodynamic model proposed by Wellman and Wilson (1968). The model predicts that porous material with larger capillaries connected to smaller ones are the most susceptible to damage (Arnold and Zehnder 1989). The pressure that builds up between two such connected pores, once crystallization takes place, is given by following the equation proposed assuming a spherical geometry (Everett 1961): $\Delta P = 2\gamma\ (1/r - 1/R)$, where ΔP = crystallization pressure (dyne/cm^2); γ = crystal solution surface tension (dyne/cm); r = smaller pore radius (cm); and R = larger pore radius. The calculation has been done following the method employed by Rossi-Manaresi and Tucci (1991). In Table 3, the porosity values calculated from MIP measurements have been reported; it can be noticed that only small variations of porosity have been detected after the treatment of the samples. In Fig. 5, it has been reported the pore size distribution of the ALM and the HLM series, which show a quite different distribution. The treatments are able to change slightly the pore distribution of the materials; this change can influence significantly the crystallization pressure. In Table 3, the values of the crystallization pressure have been reported, calculated from the pore size distributions. The treatments scarcely influence the ALM in term of crystallization pressure. On the contrary, the HLM series seem to suffer the presence of SiO_2, since treatments induce an increase in crystallization pressure (61.5 MPa), while in bare samples, the pressure is 17.0 MPa. This increase in pressure is partially compensated by the hydrophobicity induced by the treatment that reduce the amount of water absorbed by the treated sample and this lead to a lower amount of salt introduced into the stone porous structure. These two effects, higher crystallization pressure and lower amount of salt into the stone, make the bare HLM and the SiO_2 hybrid coating similar against salt weathering.

The interaction with atmospheric gases and aerosol deposition is one of the main processes of environmental degradation, occurring on the exposed surfaces of monuments and historic buildings. For this reason, both bare and treated samples have been exposed in a typical urban polluted environment at the Milan University Campus, and the concentration of the main anions (Fig. S4), typically found in degraded stones, has been monitored as in our previous work (Watt et al. 2014; Cappelletti et al. 2015b). In particular, sulphate is the main product of carbonate degradation due to pollution, whereas nitrate and chloride are mainly due to atmospheric depositions (Fuente et al. 2011; De et al. 2013). In Fig. S4, the trend of the average concentration of nitrates and sulphates is reported: the period between May 2014 and November 2015 (corresponding to the exposure time) is characterized by the highest amount of these pollutants, thus representing incisive experimental conditions. Hence, as shown in Fig. 6a, in HLM-coated samples, the overall absorption of anions was strongly reduced. Nitrates and chlorides were found in much lower concentrations than sulphates, but it is well known that sulphitation process is the main degradation reaction of calcium carbonate. Indeed, the reaction between $Ca(OH)_2$ (portlandite) and sulphuric acid, which leads to the formation of stable products (gypsum), is more favourable with respect to the reaction between portlandite and nitric acid (Cappelletti et al. 2015b). Furthermore, either nitrate or chloride concentrations were reduced with the application of both resins, with a slight further decrease for the hybrid coatings. It is also worth noting the drastic decrease in the sulphate concentrations, particularly for the hybrid BP9710 SiO_2. As previously demonstrated (Cappelletti et al. 2015b), the two pure resins BS16 and SI30 were not effective in the protection of ALM mortar and the same thing has been observed for the resin BP9710. Moreover, SI30 TiO_2 coated samples were not exposed since they did not show good UV resistance in the controlled ageing tests, which does not make them feasible candidates for environmental protection. Colorimetric measurements (CIELab) were carried out to verify the colour alteration of the protective films. The results, shown in Fig. 6b, highlight how both the BP9710 the hybrid coating containing SiO_2-coated mortars showed no significant variations in the colour, even after 7 months of exposure (only a slightly decrease of brightness has been determined). The SCA measurement showed a similar trend (see Fig. 6c): the BP9710-coated

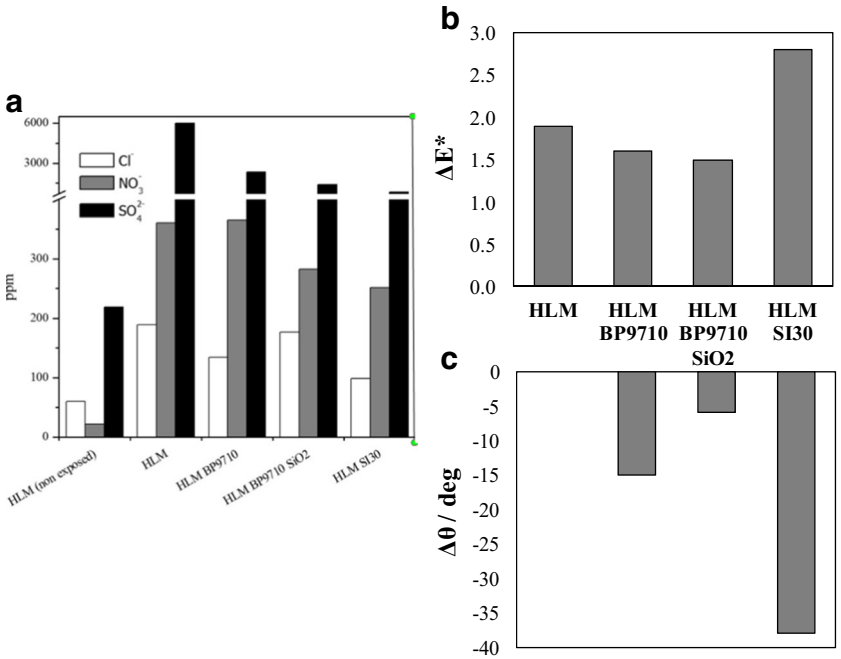

Fig. 6 **a)** Anions concentration determined by ion chromatography (IC) in HLM exposed samples, **b)** ΔE^* and **c)** static contact angle variations and after HLM sample exposure

materials retained the hydrophobic behaviour better than the SI30 ones, indicating better resistance of the water-based system, and the high performing BP9710 SiO_2 coating remained stable maintaining a high surface hydrophobicity.

In conclusion, with respect to the results previously reported in the literature for mixed coatings (Manoudis et al. 2009b), the present hybrid films are clearly more stable to outdoor exposure. Indeed, Manoudis et al. (2009b) reported a reduction of the static contact angle values of about 12° (from 162° to 150°) for a silica/siloxane hybrid, whereas in the present study BP9710, SiO_2 has shown a very small decrease (i.e. 5°; Fig. 6c), hence underlining the preservation of highly hydrophobic surfaces.

Conclusions

In the present work, two already characterized artificial stones (Cappelletti et al. 2015b), an air-hardening calcic lime mortar (ALM) and a natural hydraulic lime mortar (HLM), were used.

Alpha®SI30 and Bluesil®BP9710 resins were applied to the bare mortars to give hydrophobic features; these Si-based polymers were used as base to prepare hybrid organic–inorganic coatings, through the addition of oxide nanoparticles. Comparing the commercial polymers with the modified ones, the latter shows better features in hydrophobicity, transpirability and capillarity rinse. Although, SI30 TiO_2 shows lower chemical stability after UV and QUV ageing (higher ΔE^* values and appreciable contact angle lowering) with respect to the relative commercial resin. On the contrary, the hybrid coating BP9710 SiO_2 shows promising ageing resistance, comparable with BP9710, retaining its superior characteristic in terms of water protection. Salts crystallization resistance tests were carried out, and the final performances of the coatings in terms of reduction of salts formation (i.e. sulfate and nitrate formation) were studied after a prolonged exposure to a polluted environment (Unimi Campus in Milan). All of the treated samples show a reduction in terms of both nitrates and sulphates formation. The combined effect of these factors indicates that BP9710 modified with the addition of SiO_2 nanoparticles seems to be a novel promising protective coating agent in the field of historical building reconstruction. The results obtained have shown that HLM samples coated with the hybrid systems achieved superhydrophobicity. In particular, the water-based system shows promising results, being ecofriendly, invisible to naked eye, superhydrophobic and ageing resistant.

References

Arnold A, Zehnder K (1989) Proc. 1st Int. Symposium on the Conservation of Monuments in the Mediterranean Basin. Bari, p 31–58

Bortolotti V, Camaiti M, Casieri C, et al. (2006) Water absorption kinetics in different wettability conditions studied at pore and sample scales in porous media by NMR with portable single-sided and laboratory imaging devices. J Magn Reson 181:287–295. doi:10.1016/j.jmr.2006.05.016

Cappelletti G, Fermo P (2016) Hydrophobic and superhydrophobic coatings for limestone and marble conservation. In: M. F. Montemor (ed) Smart composite coatings and membranes: transport, structural, environmental and energy applications. Elsevier, p 490

Cappelletti G, Ardizzone S, Meroni D, et al. (2013) Wettability of bare and fluorinated silanes: a combined approach based on surface free energy evaluations and dipole moment calculations. J Colloid Interface Sci 389:284–291. doi:10.1016/j.jcis.2012.09.008

Cappelletti G, Fermo P, Camiloni M (2015a) Smart hybrid coatings for natural stones conservation. Prog Org Coat 78:511–516

Cappelletti G, Fermo P, Pino F, et al. (2015b) On the role of hydrophobic Si-based protective coatings in limiting mortar deterioration. Environ Sci Pollut Res:1–11. doi:10.1007/s11356-015-4962-0

Caruso F, Maria A, Sanchez A, et al. (2014) Chemomechanics of salt damage in stone. Nat Commun 5:1–5. doi:10.1038/ncomms5823

Chatzigrigoriou A, Manoudis PN, Karapanagiotis I (2013) Fabrication of water repellent coatings using waterborne resins for the protection of the cultural heritage. Macromol Symp:331–332. doi:10.1002/masy.201300063

De Ferri L, Lottici PP, Lorenzi A, et al. (2011) Study of silica nanoparticles—polysiloxane hydrophobic treatments for stone-based monument protection. J Cult Herit 12:356–363. doi:10.1016/j.culher.2011.02.006

De Fuente D, Vega JM, Viejo F, et al. (2011) City scale assessment model for air pollution effects on the cultural heritage. Atmos Environ 45:1242–1250. doi:10.1016/j.atmosenv.2010.12.011

De D, Manuel J, Viejo F, et al. (2013) Mapping air pollution effects on atmospheric degradation of cultural heritage. J Cult Herit 14:138–145. doi:10.1016/j.culher.2012.05.002

Doehne E, Price CA (2010) Stone conservation, an overview of current research. Getty Publication, Los Angeles

Esposito Corcione C, Striani R, Frigione M (2014) Novel hydrophobic free-solvent UV-cured hybrid organic-inorganic methacrylic-based coatings for porous stones. Prog Org Coat 77:803–812. doi:10.1016/j.porgcoat.2014.01.008

Everett DH (1961) The thermodynamics of frost damage to porous solids. Trans Faraday Soc 57:1541–1551

Fedor GR, Brennan PJ (1996) Technical bulletin LU-8035, comparison between natural weathering and fluorescent uv exposures: UVA-340 lamp test results. 1–12

Fermo P, Cappelletti G, Cozzi N, Padeletti G (2014) Hydrophobizing coatings for cultural heritage. A detailed study of resin/stone surface interaction. Appl Phys A Mater Sci Process 116:341–348

Flatt RJ (2002) Salt damage in porous materials: how high supersaturations are generated. J Cryst Growth 242:435–454. doi:10.1016/S0022-0248(02)01429-X

Fujishima A, Zhang X, Tryk DA (2008) TiO_2 photocatalysis and related surface phenomena. Surf Sci Rep 63:515–582. doi:10.1016/j.surfrep.2008.10.001

Goffredo G (2013) Smart surfaces for architectural heritage: self-cleaning titanium dioxide nano-coatings on travertine. Dissertation, Università Politecnica delle Marche

Irie H, Kamiya K, Shibanuma T, et al. (2009) Visible light-sensitive Cu(II)-grafted TiO_2 photocatalysts: activities and X-ray absorption fine structure analyses. J Phys Chem C 113:10761–10766. doi:10.1021/jp903063z

Karapanagiotis I, Pavlou A, Manoudis PN, Aifantis KE (2014) Water repellent ORMOSIL films for the protection of stone and other materials. Mater Lett 131:276–279. doi:10.1016/j.matlet.2014.05.163

Kaur K, Singh CV (2012) Amorphous TiO_2 as a photocatalyst for hydrogen production: a DFT study of structural and electronic properties. Energy Procedia 29:291–299. doi:10.1016/j.egypro.2012.09.035

La Russa MF, Ruffolo, SA, Rovella N, et al (2012) Multifunctional TiO_2 coatings for cultural heritage. Prog Org Coat 74:186–191. doi:10.1016/j.porgcoat.2011.12.008

Maino G, Meroni D, Pifferi V, et al. (2013) Electrochemically assisted deposition of transparent, mechanically robust TiO_2 films for advanced applications. J Nanopart Res. doi:10.1007/s11051-013-2087-2

Manoudis PN, Karapanagiotis I, Tsakalof A, et al. (2009a) Superhydrophobic films for the protection of outdoor cultural heritage assets. Appl Phys A Mater Sci Process 97:351–360. doi:10.1007/s00339-009-5233-z

Manoudis PN, Tsakalof A, Karapanagiotis I, et al. (2009b) Fabrication of super-hydrophobic surfaces for enhanced stone protection. Surf Coatings Technol 203:1322–1328. doi:10.1016/j.surfcoat.2008.10.041

Morikawa T, Irokawa Y, Ohwaki T (2006) Enhanced photocatalytic activity of TiO_2-xN_x loaded with copper ions under visible light irradiation. Appl Catal A Gen 314:123–127. doi:10.1016/j.apcata.2006.08.011

Ohtani B (2010) Photocatalysis A to Z—what we know and what we do not know in a scientific sense. J Photochem Photobiol C Photochem Rev 11:157–178. doi:10.1016/j.jphotochemrev.2011.02.001

Owens DKWR (1969) Estimation of the surface free energy of polymers. J Appl Polym Sci 13:1741–1747. doi:10.1592/phco.30.10.1004

Quagliarini E, Bondioli F, Goffredo GB, et al. (2012) Smart surfaces for architectural heritage: preliminary results about the application of TiO_2-based coatings on travertine. J Cult Herit 13:204–209. doi:10.1016/j.culher.2011.10.002

Rodrigues JD, Grossi a. (2007) Indicators and ratings for the compatibility assessment of conservation actions. J Cult Herit 8:32–43. doi:10.1016/j.culher.2006.04.007

Rossi-Manaresi R, Tucci A (1991) Pore structure and the disruptive or cementing effect of salt crystallization in various types of stone. Stud Conserv 36:53–58

Ruffolo SA, La Russa MF, Aloise P, et al. (2014) Efficacy of nanolime in restoration procedures of salt weathered limestone rock. Appl Phys A Mater Sci Process 114:753–758. doi:10.1007/s00339-013-7982-y

Technical Bulletin (1993) Irradiance control in fluorescent uv exposure testers. 4:1–8, Q-LAB Corporation, USA

Technical Bulletin LU-8010 (1987) Controlled irradiance in laboratory weathering: limitation in the state of the art. 1–8, Q-LAB Corporation, USA

Toniolo L, Boriani M, Guidi G (2015) Built heritage: monitoring conservation management. Springer, 442 pages

UNI EN 15801 (2010) Conservation of cultural property—test methods—determination of water absorption by capillarity

UNI EN 15803 (2009) Conservation of cultural property—test methods—determination of water vapour permeability

Watt J, Tidblad J, Kucera V, Hamilton R (2014) The effect of air pollution on cultural heritage. Springer, New York

Wellman HW, Wilson AT (1968) Salt weathering or fretting. In: Fairbridge RW (ed) Encyclopedia of geomorphology. Dowden, Hutchinson & Ross, Stroudsburg, PA, p 968–970

Wicks ZW Jr (2007) Organic coatings, Third ed. Wiley&Sons

Yu S, Oguchi C (2010) Role of pore size distribution in salt uptake, damage, and predicting salt susceptibility of eight types of Japanese building stones. Eng Geol 115:226–236

Zielecka M, Bujnowska E (2006) Silicone-containing polymer matrices as protective coatings: properties and applications. Prog Org Coat 55:160–167. doi:10.1016/j.porgcoat.2005.09.012